Figure 6. Distribution of DDX3 and IPS-1. (A) DDX3 colocalizes with IPS-1 on the mitochondria in Oc cells. HA-tagged DDX3 and FLAG-tagged IPS-1 were co-transfected into Oc cells. After 24 hrs, cells were fixed with formaldehyde and stained with anti-HA polyclonal and FLAG monoclonal Abs. Alexa488 (DDX3-HA) or Alexa633 antibody was used for second antibody. Mitochondria were stained with Mitotracker Red. Similar IPS-1-DDX3 merging profiles were observed in Huh7.5.1 cells (Fig. S3). (B,C) O cells with the HCV replicon poorly formed the DDX3-IPS-1 complex. Plasmids carrying IPS-1 (100 ng) or DDX3 (150 or 300 ng) were transfected into O (HCV replicon +) as in Oc cells (no replicon, panel A). After 24 hrs, localization of IPS-1 and DDX3 was examined by confocal microscopy. Two representatives which differ from the conventional profile (as in panel A) are shown. Similar sets of experiments were performed four times to confirm the results.
doi:10.1371/journal.pone.0014258.g006

(Fig. S2A). MDA5-dependent IFN-beta promoter activation was also suppressed by the core expression (Fig. S2B). The inhibitory effect of the core protein on DDX3-IPS-1 interaction was further confirmed using an 1b core isoform isolated from a patient. This HCV core protein also reduced interaction as well as IPS-1-mediated IFN-beta promoter activation (Fig. 5A). The blocking effect was relatively weak in cells expressing IPS-1 and full-length DDX3 (Fig. 5B). We presume that this is because there are multiple binding sites for IPS-1 in the DDX3 whole molecule [11]. For binding assay, we used DDX3 2-3c (across a.a. 199~662, longer than 224~662) instead of the whole DDX3. In fact, DDX3(199-662)-IPS-1 interaction was blocked by the additional expression of core protein (HCVO, JFH1 or 1b core) in Fig. 5C. Ultimately, HCV core protein suppresses IPS-1 signaling by blocking the interaction between the C-terminal region of DDX3 and the CARD-like region of IPS-1, and this inhibition apparently causes the disruption of the active RIG-I/DDX3/IPS-1 complex that efficiently induces IFN-beta production signaling.

Localization of DDX3 and HCV core protein in O cells

We attempted to confirm this finding by tag-expressed proteins and imaging analysis. In Huh7.5 cells IPS-1 colocalized with DDX3 around the mitochondria (Fig. S3), and so did in the hepatocyte lines Oc cells with no HCV replicon (Fig. 6A). In Oc and Huh7.5.1 cells with no HCV replicon, abnormal distribution of IPS-1 was barely observed (Fig. 6A, Fig. S3). In O cells expressing DDX3 and IPS-1, by contrast, two distinct profiles of IPS-1 were observed in addition to the Fig. 6A pattern of IPS-1: diminution or spreading of the IPS-1 protein over mitochondria (Fig. 6B,C). IPS-1 may be degraded by NS3/4A in some replicon-expressing O cells as reported previously [5,28]. We counted number of cells having the pattern represented by Fig. 6 panel B and those similar to Fig. 6 panel C, and in most cases the latter patterns were predominant.

What happens in the O cells with replicon when the core protein is expressed was next tested. Using O and Oc cells, we tested the localization of the core protein and DDX3 in comparison with IFN-inducing properties (Fig. 3). In O cells with full-length HCV replicon, DDX3 was localized proximal to the lipid droplets (LD) (Fig. 7A top panel) around which HCV particles assembled [29]. HCV core protein and DDX3 were partly colocalized in the HCV replicon-expressing cells (Fig. 7A center panel). The results were confirmed with HCV replicon-expressing O cells where endogenous core and DDX3 were stained (Fig. 7B upper panel). Partial merging between core and DDX3 was reproduced in this case, too. In contrast, sO cells, which possess a subgenomic replicon lacking the cording region of the core protein, showed no merging profile of DDX3 and LD (Fig. 7A bottom panel). Likewise, Oc cells barely formed assembly consisting of LD (where the core assembles) and overexpressed DDX3 (Fig. 7A bottom panel) or endogenous DDX3 (Fig. 7B lower panel). O cells expressing DDX3 tended to form large spots compared to Oc cells (with no replicon) and sO cells (core-less replicon) with DDX3.

Overexpressed DDX3 allowed the Oc cells to induce IPS-1-mediated IFN-beta promoter activation (Fig. 3B), while this failed to happen in O cells having HCV replicon (Fig. 3A). Ultimately, overexpressed IPS-1 did not facilitate efficient merging with DDX3 in O cells with replicon (Fig. 6B,C) compared to Oc cells or Huh7.5 cells with no replicon (Fig. 6A, Fig. S3). The results on the functional and immnoprecipitation analyses, together with the imaging profiles, infer that the IPS-1-enhancing function of DDX3 should be blocked by both NS3/4A-mediated IPS-1 degradation and the HCV core which translocates DDX3 from the IPS-1 complex to the proximity of LD in HCV replicon-expressing cells.

Discussion

We investigated the effect of the HCV core protein on the cytosolic DDX3 that forms a complex with IPS-1 to enhance the RIG-I-mediated RNA-sensing pathway. We demonstrated that the core protein removes DDX3 from the IFN-β-inducing complex, leading to suppression of IFN-β induction. DDX3 is functionally complex, since its protective role against viruses may be modulated by the synthesis of viral proteins. DDX3 acts on multiple steps in the IFN-inducing pathway [30]. In addition, DDX3 interacts with the HCV core protein in HCV-infected cells and promotes viral replication [16]. This alternative function is accelerated by the HCV core protein, resulting in augmented HCV propagation [14,16]. More recently, Patal et al., reported that interaction of DDX3 with core protein is not critical for the support of viral replication by DDX3, although DDX3 and core protein colocalize with lipid droplet [15]. If this is the case, what function is revealed by the interaction between DDX3 and HCV core protein remain unsettled. At least, HCV replication is not blocked by this molecular interaction [15].

It remains unclear in Fig. 4C why higher doses of JFH1 core protein are required to inhibit enhancement of IPS-1 signaling by endogenous DDX3 than by exogenously overexpressed DDX3. One possibility is that endogenous DDX3 is preoccupied in a molecular complex other than the IPS-1 pathway since DDX3 is involved in almost every step of RNA metabolism and its localization affects its functional profile [18,30].

Together with these findings, the results presented here suggest that the HCV core inactivates IPS-1 in a mode different from NS3/4A [5,31]. The core protein may switch DDX3 from an antiviral mode to an HCV propagation mode. The core protein localizes to the N-terminus of the HCV translation product, and is generated in infected cells before NS3/4A proteolytically liberates non-structural proteins and inactivates IPS-1. Our results on how the HCV core protein interferes with the interaction between DDX3 and IPS-1 add several possibilities to notions about the HCV function on the IFN-beta-inducing pathway [18].

DDX3 appears to be a prime target for viral manipulation, since at least three different viruses, including HCV [14], Hepatitis B virus [32], and poxviruses [8], encode proteins that interact with DDX3 and modulate its function. These viruses seem to co-opt DDX3, and also require it for replication. The viruses are all oncogenic, and may confer oncogenic properties to DDX3.

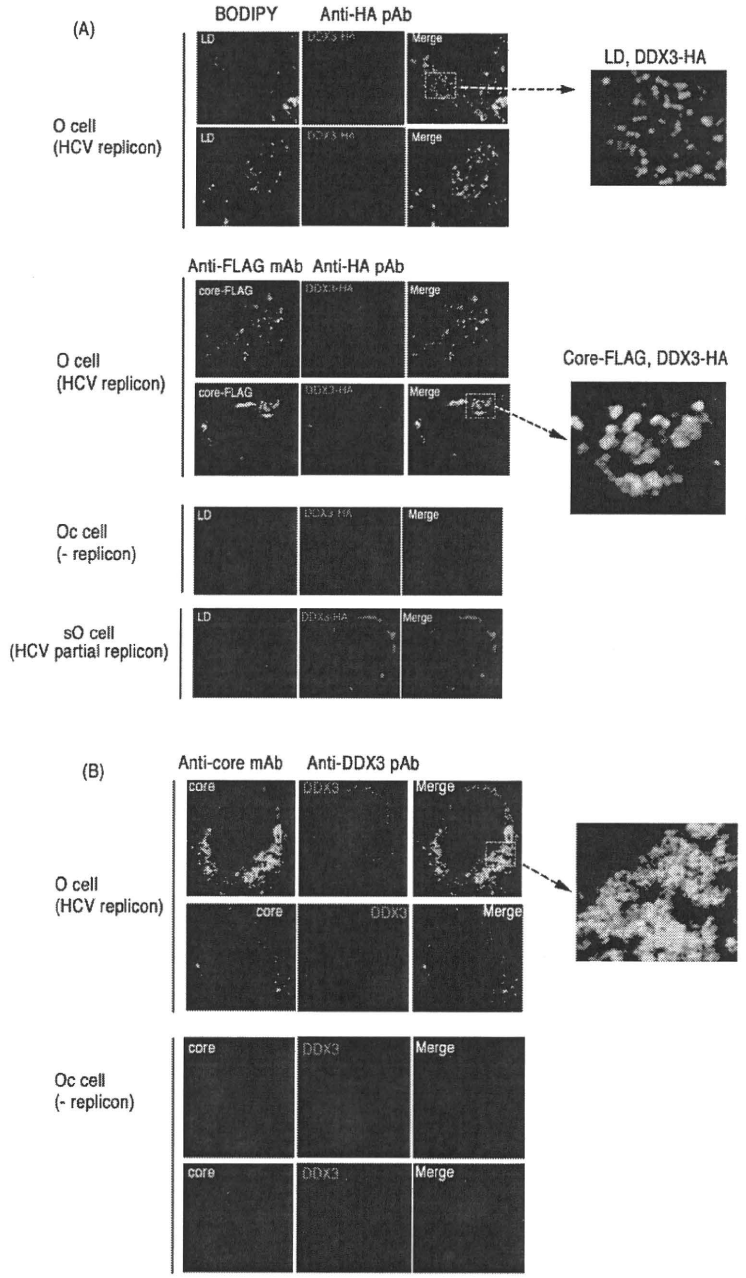

Figure 7. Partial association of endogenous and overexpressed DDX3 with HCV core protein in hepatocyte lines. (A) O cells with the HCV replicon form DDX3-containing speckles in the cytoplasm. O cells contain full-length HCV replicon, and Oc cells do not [16]. O cells were transfected with a plasmid expressing HA-tagged DDX3 (top panel). In other experiments, O cells were transfected with plasmids expressing HA-tagged DDX3 and FLAG-tagged HCV core protein (center panel). After 24 hrs, cells were stained with anti-HA or FLAG antibodies. Proteins were visualized with Alexa488 or 564 second antibodies and the LD was stained with BODIPY493/503. In the bottom panel, Oc cells (no replicon) and sO cells with the core-less subgenomic replicon [16] were transfected with a plasmid expressing HA-tagged DDX3. After 24 hrs, cells were stained with anti-HA antibodies. LD was stained with BODIPY493/503. (B) Endogenous DDX3-HCV core association in O cells. O or Oc cells were cultured to amplify the HCV replicon. Cells were stained with anti-core mAb and anti-DDX3pAb and secondary antibodies. Similar sets of experiments were performed three times to confirm the results.
doi:10.1371/journal.pone.0014258.g007

DDX3 is also involved in human immunodeficiency virus RNA translocation [33]. The DDX3 gene is conserved among eukaryotes, and includes the budding yeast homolog, Ded1 [34]. The Ded1 helicase is essential for initiation of host mRNA translation, and human DDX3 complements the lethality of Ded1 null yeast [14,35]. Another function of DDX3 is to bind viral RNA to modulate RNA replication and translocation. Constitutive expression of the HCV core or other DDX3-binding proteins may impede IFN induction and promote cell cycle progression. These reports are consistent with the implication of DDX3 in various steps of RNA metabolism in cells that contain both host and viral RNAs.

A continuing question is the physiological role of the molecular complex of DDX3 and IPS-1 during replication of HCV in hepatocytes. HCV proteins generated in host hepatocytes usually induce an HCV-permissive state in patients, for example in the IFN-inducing pathways. NS3/4A protease induces rapid degradation of IPS-1 [5,31] and TICAM-1/TRIF [36]. NS5A interferes with the MyD88 function [37]. Viral replication ultimately blocks the STAT1-mediated IFN-amplification pathway [38]. PKR may be an additional factor by which HCV controls type I IFN production [39]. Our results add to our knowledge of the mechanism of how HCV circumvents IFN induction in host cells: HCV core protein suppresses the initial step of IFN-beta induction by interfering with DDX3-IPS-1 association. Indeed, the core protein functions as the earliest IFN suppressor, since it is generated first in HCV-infected cells, and rapidly couples with DDX3 to retract it from the IPS-1 complex, resulting in localization of DDX3 near the LD (Fig. 7). It is HCV that hijacks this protein for establishing infection. Although gene disruption of DDX3 makes mice lethal, this issue will be further tested using IPS-1 $-/-$ hepatocytes expressing human CD81 and occludin [40], in which HCV replication would proceed.

DDX3 primarily is an accelerating factor for antiviral response through IPS-1-binding. Many host proteins other than DDX3 may positively regulate HCV replication in hepatocytes in association with the IPS-1 pathway. In this context, we know LGP2 [41] and STING [42] act as positive regulators in virus infection. Peroxisomes serve as signaling platforms for recruiting IPS-1 with a different signalosome than mitochondria [43]. It appears rational that HCV harbors strategies to circumvent these positive regulators in the relevant steps of the IFN-inducing pathway.

Imaging studies suggest that the complex of IPS-1 involving the membrane of mitochondrial/peroxisomes differ from that free from the membrane. Although IPS-1 is liberated from the membrane by NS3/4A having largely intact cytosolic domain, it loses the IFN-inducing function [5,31]. Our results could offer the possibility that the clipped-out form of IPS-1 immediately fails to form the conventional complex for IRF-3 activation any more [44] or is easily degraded further to be inactive (Fig. 6C). Indeed, there are a number of mitochondria-specific molecules which assemble with IPS-1 [45]. Formation of the molecular complex on the mitochondria rather than simple association between IPS-1 and DDX3 may be critical for the DDX3 function.

Evidence is accumulating that HCV checks many steps in the IFN-inducing pathway throughout the early and late infection stages, and suppresses IFN production by multiple means. Disruption of IPS-1 function by both NS3/4A and core protein may be crucial in HCV-infected Huh7.5 cells, even though the cells harbor dysfunctional RIG-I [46]. Type I IFN suppresses tumors by causing expression of p53 and other tumor-suppressing agents [47]. These unique features of the HCV core protein require further confirmation, and should be minded in investigation of HCV persistency, chronic infection and progression to cirrhosis and carcinoma.

Supporting Information

Figure S1 The IPS-1 complex. IPS-1 and HCV core bind C-terminal regions of DDX3. DDX3 captures dsRNA at the C-terminal domain. This figure is constructed from [11], [14] and [16].
Found at: doi:10.1371/journal.pone.0014258.s001 (0.41 MB TIF)

Figure S2 DDX3 enhances RIG-I-mediated IFN-β promoter activation induced by polyI:C. (A) DDX3 si-1 or control siRNA was transfected into HEK293 cells with reporter plasmids and RIG-I-expression plasmid or control plasmid (100 ng). After 48 hrs, cells were stimulated with polyI:C (20 μg/ml) with dextran for 4 hrs, and activation of the reporter p125luc was measured. (B) MDA5 (25 ng), IPS-1 (100 ng), DDX3 (100 ng), JFH1 core (50 ng) and/or p125 luc reporter (100 ng) plasmids were transfected with HEK293 cells. Cell lysates were prepared after 24 hrs, and luciferase activities measured. The results are representative of two independent experiments, each performed in triplicate.
Found at: doi:10.1371/journal.pone.0014258.s002 (0.17 MB TIF)

Figure S3 DDX3 colocalizes with IPS-1 on the mitochondria in Huh7.5.1 cells. HA-tagged DDX3 and FLAG-tagged IPS-1 were co-transfected into Huh7.5.1 cells. After 24 hrs, cells were fixed with formaldehyde and stained with anti-HA polyclonal and FLAG monoclonal Abs. Alexa488 (DDX3-HA) or Alexa633 antibody was used for second antibody. Mitochondria were stained with Mitotracker Red. A representative result from three independent experiments is shown.
Found at: doi:10.1371/journal.pone.0014258.s003 (0.92 MB TIF)

Acknowledgments

We thank Drs. Y. Matsuura (Osaka Univ.), Kyoko Mori (Okayama Univ.), and M. Sasai (Yale Univ.) for invaluable discussions. Thanks are also due to Drs. T. Ebihara, K. Funami, A. Matsuo, A. Ishii, and M. Shingai in our laboratory for their critical discussions.

Author Contributions

Conceived and designed the experiments: HO MM TS. Performed the experiments: HO MM. Analyzed the data: HO MM KS TS. Contributed reagents/materials/analysis tools: MI AW OT SA NK KS. Wrote the paper: HO TS.

References

1. Yoneyama M, Kikuchi M, Natsukawa T, Shinobu N, Imaizumi T, et al. (2004) The RNA helicase RIG-I has an essential function in double-stranded RNA-induced innate antiviral responses. Nat Immunol 5: 730–737.
2. Yoneyama M, Kikuchi M, Matsumoto K, Imaizumi T, Miyagishi M, et al. (2005) Shared and unique functions of the DExD/H-box helicases RIG-I, MDA5, and LGP2 in antiviral innate immunity. J Immunol 175: 2851–2858.
3. Kato H, Takeuchi O, Sato S, Yoneyama M, Yamamoto M, et al. (2006) Differential roles of MDA5 and RIG-I helicases in the recognition of RNA viruses. Nature 441: 101–105.
4. Kawai T, Takahashi K, Sato S, Coban C, Kumar H, et al. (2005) IPS-1, an adaptor triggering RIG-I- and Mda5-mediated type I interferon induction. Nat Immunol 6: 981–988.

5. Meylan E, Curran J, Hofmann K, Moradpour D, Binder M, et al. (2005) Cardif is an adaptor protein in the RIG-I antiviral pathway and is targeted by hepatitis C virus. Nature 437: 1167–1172.
6. Seth RB, Sun L, Ea CK, Chen ZJ (2005) Identification and characterization of MAVS, a mitochondrial antiviral signaling protein that activates NF-kappaB and IRF 3. Cell 122: 669–682.
7. Xu LG, Wang YY, Han KJ, Li LY, Zhai Z, et al. (2005) VISA is an adapter protein required for virus-triggered IFN-beta signaling. Mol Cell 19: 727–740.
8. Schroder M, Baran M, Bowie AG (2008) Viral targeting of DEAD box protein 3 reveals its role in TBK1/IKKepsilon-mediated IRF activation. Embo J 27: 2147–2157.
9. Soulat D, Bürckstümmer T, Westermayer S, Goncalves A, Bauch A, et al. (2008) The DEAD-box helicase DDX3X is a critical component of the TANK-binding kinase 1-dependent innate immune response. Embo J 27: 2135–2146.
10. Kravchenko VV, Mathison JC, Schwamborn K, Mercurio F, Ulevitch RJ (2003) IKKi/IKKepsilon plays a key role in integrating signals induced by pro-inflammatory stimuli. J Biol Chem 278: 26612–26619.
11. Oshiumi H, Sakai K, Matsumoto M, Seya T (2010) DEAD/H BOX 3 (DDX3) helicase binds the RIG-I adaptor IPS-1 to up-regulate IFN-beta inducing potential. Eur J Immunol 40: 940–948.
12. Chao CH, Chen CM, Cheng PL, Shih JW, Tsou AP, et al. (2006) A DEAD box RNA helicase with tumor growth-suppressive property and transcriptional regulation activity of the p21waf1/cip1 promoter, is a candidate tumor suppressor. Cancer Res 66: 6579–6588.
13. Rocak S, Linder P (2004) DEAD-box proteins: the driving forces behind RNA metabolism. Nat Rev Mol Cell Biol 5: 232–241.
14. Owsianka AM, Patel AH (1999) Hepatitis C virus core protein interacts with a human DEAD box protein DDX3. Virology 257: 330–340.
15. Angus AGN, Dalrymple D, Boulant S, McGivern DR, Clayton RF, et al. (2010) Requirement of cellular DDX3 for hepatitis C virus replication is unrelated to its interaction with the viral core protein. J Gen Virol 91: 122–132.
16. Ariumi Y, Kuroki M, Abe K, Dansako H, Ikeda M, et al. (2007) DDX3 DEAD-box RNA helicase is required for hepatitis C virus RNA replication. J Virol 81: 13922–13926.
17. Chang PC, Chi CW, Chau GY, Li FY, Tsai YH, et al. (2006) DDX3, a DEAD box RNA helicase, is deregulated in hepatitis virus-associated hepatocellular carcinoma and is involved in cell growth control. Oncogene 25: 1991–2003.
18. Schroder M (2010) Human DEAD-box protein 3 has multiple functions in gene regulation and cell cycle control and is a prime target for viral manipulation. Biochem Pharmacol 79: 297–306.
19. Ikeda M, Abe K, Dansako H, Nakamura T, Naka K, et al. (2005) Efficient replication of a full-length hepatitis C virus genome, strain O, in cell culture, and development of a luciferase reporter system. Biochem Biophys Res Commun 329: 1350–1359.
20. Lin W, Kim SS, Yeung E, Kamegaya Y, Blackard JT, et al. (2006) Hepatitis C virus core protein blocks interferon signaling by interaction with the STAT1 SH2 domain. J Virol 2006 Sep; 80(18): 9226–35.
21. Sasai M, Shingai M, Funami K, Yoneyama M, Fujita T, et al. (2006) NAK-associated protein 1 participates in both the TLR3 and the cytoplasmic pathways in type I IFN induction. J Immunol 177: 8676–8683.
22. Oshiumi H, Matsumoto M, Funami K, Akazawa T, Seya T (2003) TICAM-1, an adaptor molecule that participates in Toll-like receptor 3-mediated interferon-beta induction. Nat Immunol 4: 161–167.
23. Saito T, Owen DM, Jiang F, Marcotrigiano J, Gale M, Jr. (2008) Innate immunity induced by composition-dependent RIG-I recognition of hepatitis C virus RNA. Nature 454: 523–527.
24. Saito T, Hirai R, Loo YM, Owen D, Johnson CL, et al. (2007) Regulation of innate antiviral defenses through a shared repressor domain in RIG-I and LGP2. Proc Natl Acad Sci U S A 104: 582–587.
25. Matsumoto M, Funami K, Tanabe M, Oshiumi H, Shingai M, et al. (2003) Subcellular localization of Toll-like receptor 3 in human dendritic cells. J Immunol 171: 3154–3162.
26. Oshiumi H, Matsumoto M, Hatakeyama S, Seya T (2009) Riplet/RNF135, a RING finger protein, ubiquitinates RIG-I to promote interferon-beta induction during the early phase of viral infection. J Biol Chem 284: 807–817.
27. Schwer B, Ren S, Pietschmann T, Kartenbeck J, Kaehlcke K, et al. (2004) Targeting of hepatitis C virus core protein to mitochondria through a novel C-terminal localization motif. J Virol 78: 7958–7968.
28. Cheng G, Zhong J, Chisari FV (2006) Inhibition of dsRNA-induced signaling in hepatitis C virus-infected cells by NS3 protease-dependent and -independent mechanisms. Proc Natl Acad Sci U S A 103: 8499–8504.
29. Miyanari Y, Atsuzawa K, Usuda N, Watashi K, Hishiki T, et al. (2007) The lipid droplet is an important organelle for hepatitis C virus production. Nat Cell Biol 9: 1089–1097.
30. Mulhern O, Bowie AG (2010) Unexpected roles for DEAD-box protein 3 in viral RNA sensing pathways. Eur J Immunol 40: 933–935.
31. Li XD, Sun L, Seth RB, Pineda G, Chen ZJ (2005) Hepatitis C virus protease NS3/4A cleaves mitochondrial antiviral signaling protein off the mitochondria to evade innate immunity. Proc Natl Acad Sci U S A 102: 17717–17722.
32. Wang H, Kim S, Ryu WS (2009) DDX3 DEAD-Box RNA helicase inhibits hepatitis B virus reverse transcription by incorporation into nucleocapsids. J Virol 83: 5815–5824.
33. Yedavalli VS, Neuveut C, Chi YH, Kleiman L, Jeang KT (2004) Requirement of DDX3 DEAD box RNA helicase for HIV-1 Rev-RRE export function. Cell 119: 381–392.
34. Chuang RY, Weaver PL, Liu Z, Chang TH (1997) Requirement of the DEAD-Box protein ded1p for messenger RNA translation. Science 275: 1468–1471.
35. Mamiya N, Worman HJ (1999) Hepatitis C virus core protein binds to a DEAD box RNA helicase. J Biol Chem 274: 15751–15756.
36. Li K, Foy E, Ferreon JC, Nakamura M, Ferreon AC, et al. (2005) Immune evasion by hepatitis C virus NS3/4A protease-mediated cleavage of the Toll-like receptor 3 adaptor protein TRIF. Proc Natl Acad Sci U S A 102: 2992–2997.
37. Abe T, Kaname Y, Hamamoto I, Tsuda Y, Wen X, et al. (2007) Hepatitis C virus nonstructural protein 5A modulates the toll-like receptor-MyD88-dependent signaling pathway in macrophage cell lines. J Virol 81: 8953–8966.
38. Heim MH, Moradpour D, Blum HE (1999) Expression of hepatitis C virus proteins inhibits signal transduction through the Jak-STAT pathway. J Virol 73: 8469–8475.
39. Arnaud N, Dabo S, Maillard P, Budkowska A, Kalliampakou KI, et al. (2010) Hepatitic C virus controls interferon production through PKR activation. PLoS One 5: e10575.
40. Ploss A, Evans MJ, Gaysinskaya VA, Panis M, You H, et al. (2009) Human occludin is a hepatitis C virus entry factor required for infection of mouse cells. Nature 457: 882–886.
41. Satoh T, Kato H, Kumagai Y, Yoneyama M, Sato S, et al. (2010) LGP2 is a positive regulator of RIG-I- and MDA5-mediated antiviral responses. Proc Natl Acad Sci U S A 107: 1512–1517.
42. Ishikawa H, Ma Z, Barber GN (2009) STING regulates intracellular DNA-mediated, type I interferon-dependent innate immunity. Nature 461: 788–793.
43. Dixit E, Boulant S, Zhang Y, Lee ASY, Odendall C, et al. (2010) Peroxisomes are signaling platforms for antiviral innate immunity. Cell 141: 668–681.
44. Yasukawa K, Oshiumi H, Takeda M, Ishihara N, Yanagi Y, et al. (2009) Mitofusin 2 inhibits mitochondrial antiviral signaling. Sci Signal 2: ra47.
45. Scott I (2010) The role of mitochondria in the mammalian antiviral defense system. Mitochondrion 10: 316–320.
46. Binder M, Kochs G, Bartenschlager R, Lohmann V (2007) Hepatitis C virus escape from the interferon regulatory factor 3 pathway by a passive and active evasion strategy. Hepatology 46: 1365–1374.
47. Takaoka A, Yanai H, Kondo S, Duncan G, Negishi H, et al. (2005) Integral role of IRF-5 in the gene induction programme activated by Toll-like receptors. Nature 434: 243–249.

Hepatology Research

Hepatology Research 2010; **40**: 1248–1253 doi: 10.1111/j.1872-034X.2010.00730.x

Short Communication

Gene expression profile of Li23, a new human hepatoma cell line that enables robust hepatitis C virus replication: Comparison with HuH-7 and other hepatic cell lines

Kyoko Mori,* Masanori Ikeda, Yasuo Ariumi and Nobuyuki Kato*

Department of Tumor Virology, Okayama University Graduate School of Medicine, Dentistry and Pharmaceutical Sciences, Okayama, Japan

Aim: Human hepatoma cell line HuH-7-derived cells are currently the only cell culture system used for robust hepatitis C virus (HCV) replication. We recently found a new human hepatoma cell line, Li23, that enables robust HCV replication. Although both cell lines had similar liver-specific expression profiles, the overall profile of Li23 seemed to differ considerably from that of HuH-7. To understand this difference, the expression profile of Li23 cells was further characterized by a comparison with that of HuH-7 cells.

Methods: cDNA microarray analysis using Li23 and HuH-7 cells was performed. Li23-derived ORL8c cells and HuH-7-derived RSc cells, in which HCV could infect and efficiently replicate, were also used for the microarray analysis. For the comparative analysis by reverse transcription polymerase chain reaction (RT–PCR), human hepatoma cell lines (HuH-6, HepG2, HLE, HLF and PLC/PRF/5) and immortalized hepatocyte cell line (PH5CH8) were also used.

Results: Microarray analysis of Li23 versus HuH-7 cells selected 80 probes to represent highly expressed genes that have ratios of more than 30 (Li23/HuH-7) or 20 (HuH-7/Li23). Among them, 17 known genes were picked up for further analysis. The expression levels of most of these genes in Li23 and HuH-7 cells were retained in ORL8c and RSc cells, respectively. Comparative analysis by RT–PCR using several other hepatic cell lines resulted in the classification of 17 genes into three types, and identified three genes showing Li23-specific expression profiles.

Conclusion: Li23 is a new hepatoma cell line whose expression profile is distinct from those of frequently used hepatic cell lines.

Key words: hepatitis C virus, hepatoma cell line, HuH-7, Li23, microarray

INTRODUCTION

HUH-7, A HUMAN hepatoma cell line,[1] is frequently used in the research of hepatitis C virus (HCV), since an HCV replicon system enabling HCV subgenomic RNA replication was developed using HuH-7 cells.[2] Even with the use of an efficient HCV production system developed in 2005,[3] HuH-7-derived cells are still used as the only cell line for persistent HCV production systems.

Correspondence: Professor Nobuyuki Kato, Department of Tumor Virology, Okayama University Graduate School of Medicine, Dentistry and Pharmaceutical Sciences, Okayama 700-8558, Japan. Email: nkato@md.okayama-u.ac.jp

*These authors contributed equally to this work.

Received 21 July 2010; revision 16 August 2010; accepted 17 August 2010.

We previously developed HCV replicon systems[4,5] and an HCV production system[6] using HuH-7-derived cells. Furthermore, we recently found a new human hepatoma cell line, Li23, that enables robust HCV RNA replication and persistent HCV production.[7] In that study, using microarray analysis, we excluded the possibility that the obtained Li23-derived cells were derived from contamination of HuH-7-derived cells used for HCV replication.[7] In addition, we noticed that the gene expression profile of Li23 cells seemed considerably different from that of HuH-7 cells. Therefore, we assumed that the Li23 cell line possesses a unique expression profile among widely used human hepatoma cell lines. To evaluate this assumption, we further characterized the expression profile of Li23 cells by comparing it with those of other human hepatoma cell lines, including HuH-7,[1] HuH-6,[8] HepG2,[9] HLE,[10] HLF[10] and PLC/PRF/5.[11] Human immortalized hepatocyte cell line

PH5CH8[12] was also used for the comparison. Here, we show that the Li23 cell line possesses a distinct expression profile among hepatic cell lines.

METHODS

Cell culture

HUH-7, HUH-6, HEPG2, HLE, HLF and PLC/PRF/5 cells were cultured in Dulbecco's modified Eagle's medium supplemented with 10% fetal bovine serum. Li23 and PH5CH8 cells were maintained as described previously.[7] Cured cells (Li23-derived ORL8c and HuH-7-derived RSc), from which the HCV RNA had been eliminated by interferon (IFN) treatment, were also maintained as described previously.[7]

cDNA microarray analysis

Li23, ORL8c, HuH-7 and RSc cells (1×10^6 each) were plated onto 10-cm diameter dishes and cultured for 2 days. Total RNA from these cells were prepared using the RNeasy extraction kit (QIAGEN, Hilden, Germany). cDNA microarray analysis was performed according to the methods described previously.[7] Differentially expressed genes were selected by comparing the arrays from Li23 and HuH-7 cells. The selected genes were further compared with the array from ORL8c or RSc cells.

Reverse transcription polymerase chain reaction

Reverse transcription polymerase chain reaction (RT-PCR) was performed to detect cellular mRNA as described previously.[13] Briefly, total RNA (2 μg) was reverse-transcribed with M-MLV reverse transcriptase (Invitrogen, San Diego, CA, USA) using an oligo dT primer (Invitrogen) according to the manufacturer's protocol. One-tenth of the synthesized cDNA was used for PCR. The primers arranged for this study are listed in Table 1. In addition, we used primer sets for New York esophageal squamous cell carcinoma 1 (NY-ESO-1), β-defensin-1 (DEFB1), lectin, galactoside-binding, soluble 3 (LGALS3)/Galectin-3, melanoma-specific antigen family A6 (MAGEA6), UDP glycosyltransferase 2 family polypeptide B4 (UGT2B4), transmembrane 4 superfamily member 3 (TM4SF3), insulin-like growth factor binding protein 2 (IGFBP2), arylacetamide deacetylase (AADAC), albumin and glyceraldehyde-3-phosphate dehydrogenase (GAPDH), as described previously.[7]

RESULTS

Genes showing pronounced differences in gene expression between Li23- and HuH-7-derived cells

WE RECENTLY ESTABLISHED several Li23-derived cell lines showing robust HCV RNA replication.[7] In convenient microarray analysis using these cell lines, we noticed that the gene expression profile of Li23 cells differed considerably from that of HuH-7 cells, and that several genes, including cancer antigens such as NY-ESO-1 and MAGEA6, were highly expressed in Li23 cells but were not expressed in HuH-7 cells.[7] However, it

Table 1 Primers used for reverse transcription polymerase chain reaction analysis

Gene (accession no.)	Direction	Nucleotide sequence (5′–3′)	Products (bp)
Cancer antigen 45, A5	Forward	TGGAGATGACCTAGAATGCAG	218
(CT45A5); NM_001007551	Reverse	CTCGTCTCATACATCTTGCTG	
Four-and-a-half LIM domain 1	Forward	GGAATCACTTACCAGGATCAG	243
(FHL1; NM_001449)	Reverse	TTTGCAGTGGAAGCAGTAGTC	
Thymosin β4, X-linked	Forward	ACCAGACTTCGCTCGTACTC	179
(TMSB4X; NM_021109)	Reverse	TCGCCTGCTTGCTTCTCCTG	
Lectin, galactoside-binding, soluble 1	Forward	CAACACCATCGTGTGCAACAG	253
(LGALS1; NM_002305)	Reverse	CAGCTGCCATGTAGTTGATGG	
Interferon-induced transmembrane protein 2	Forward	CCTCTTCATGAACACCTGCTG	184
(IFITM2; NM_006435)	Reverse	CACTGGGATGATGATGAGCAG	
Apolipoproteins A1	Forward	ACTGTGTACGTGGATGTGCTC	273
(APOA1; X02162)	Reverse	CTTCTTCTGGAAGTCGTCCAG	
α-2-HS-glycoprotein	Forward	AACCGAACTGCGATGATCCAG	248
(AHSG; NM_001622)	Reverse	TTCGACAGCATGCTCCTTCAG	
Gap junction protein-α 1	Forward	CATCTTCATGCTGGTGGTGTC	253
(GJA1; NM_000165)	Reverse	GTTTCTGTCGCCAGTAACCAG	

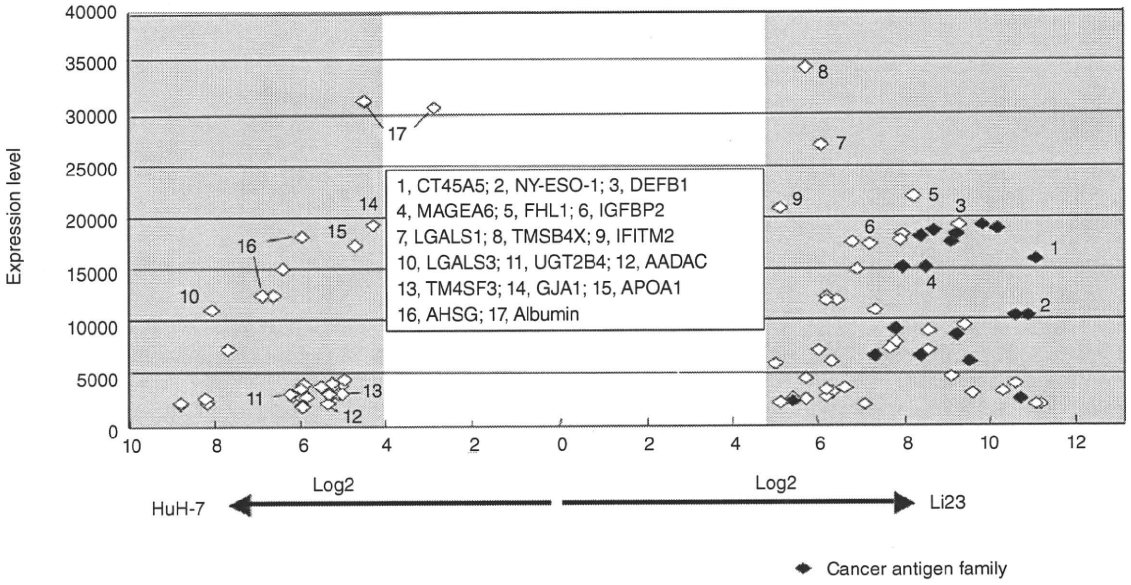

Figure 1 Genes showing pronounced differences in gene expression between Li23 and HuH-7 cells. The probes showing expression levels of more than 2000 and ratios of more than 30 (Li23/HuH-7) or 20 (HuH-7/Li23) are presented.

is unclear whether the expression profiles of these genes are characteristics of Li23 cells.

To clarify this point, comprehensive microarray analysis using Li23 and HuH-7 cells was performed. This revealed 4119 and 3570 probes whose expression levels were upregulated and downregulated at ratios of more than 2 and less than 0.5 in Li23 versus HuH-7 cells, respectively. From among these probes, we selected those showing ratios of more than 30 (Li23/HuH-7) and 20 (HuH-7/Li23), and further selected the probes showing expression levels of more than 2000 (actual value of measurement). By these selections, 80 probes were assigned (Fig. 1). The most distinguishing characteristic of the comparison is that the cancer antigen family (18 probes) was highly expressed in Li23 cells but was not highly expressed in HuH-7 cells (Fig. 1). From these probes, 14 known genes showing expression levels above 10 000 (#1–10 and #14–17 in Fig. 1) and three additional known genes (#11–13 in Fig. 1) were chosen as representative genes for further analysis.

Regarding the total of 17 genes, the expression levels in Li23 versus ORL8c or HuH-7 versus RSc were compared. The expression levels of most of the 17 genes were maintained between Li23 and ORL8c cells or between HuH-7 and RSc cells (Table 2). These results indicate that ORL8c and RSc cells retained the characteristics of parent Li23 and HuH-7 cells, respectively. However, it was notable that the expression levels of apolipoprotein A1 (APOA1), α-2-HS-glycoprotein (AHSG), and albumin were significantly higher in ORL8c cells than in Li23 cells, suggesting that ORL8c is selected as a specific clone from Li23 cell populations.

Expression profiles of representative genes whose expression levels showed drastic differences between Li23 and HuH-7 cells among human hepatic cell lines

Regarding the 17 genes selected above, we performed comparative analyses by RT-PCR using Li23, HuH-7, HuH-6, HepG2, HLE, HLF, PLC/PRF/5 and PH5CH8 cells in order to clarify whether or not these genes exhibit Li23-specific expression profiles. The results of the RT-PCR performed after optimization of PCR conditions in each gene resulted in the classification of the 17 genes into three types (A, B and C in Fig. 2). NY-ESO-1 and DEFB1 (high expression in Li23 only), and LGALS3/Galectin-3 (no expression in Li23 only) belonged to type A, which showed a Li23-specific feature. Type B showed that the expression levels in Li23, HLE, HLF, PLC/PRF/5 and/or PH5CH8 cells were greatly higher or lower than those in HuH-7, HuH-6 and HepG2 cells. Type B consisted of cancer antigen 45, A5

Table 2 Representative genes showing pronounced differences in gene expression between Li23 and HuH-7 cells

Gene	Accession no.	Li23	Li23-derived ORL8c	HuH-7	HuH-7-derived RSc
Cancer antigen 45, A5 (CT45A5)	NM_001007551	15 857†	10 508	8	23
Cancer testis antigen 1A (NY-ESO-1/CTAG1A)	U87459	9 005	5 503	5	8
β-Defensin-1 (DEFB1)	U73945	18 311	8 326	31	7
Melanoma-specific antigen family A6 (MAGEA6)	U10691	15 168	17 050	42	35
Four-and-a-half LIM domain 1 (FHL1)	NM_001449	21 851	13 428	77	79
Insulin-like growth factor binding protein 2 (IGFBP2)	NM_000597	17 429	8 931	117	13
Lectin, galactoside-binding, soluble 1 (LGALS1)	NM_002305	26 694	27 098	379	11
Thymosin β4, X-linked (TMSB4X)	NM_021109	34 273	26 199	648	307
IFN-induced transmembrane protein 2 (IFITM2)	NM_006435	20 762	9 645	595	637
Lectin, galactoside-binding, soluble 3 (LGALS3/Galectin 3)	BC001120	41	70	10 973	6 020
UDP glycosyltransferase 2 family polypeptide B4 (UGT2B4)	NM_021139	40	57	2 863	7 546
Arylacetamide deacetylase (AADAC)	NM_001086	57	73	2 282	4 746
Transmembrane 4 superfamily member 3 (TM4SF3)	NM_004616	95	51	3 220	1 265
Gap junction protein-α 43 KDa (GJA1)	NM_000165	951	2	19 090	19 485
Apolipoprotein A1 (APOA1)	X02162	673	7 230	16 920	15 202
α-2-HS-glycoprotein (AHSG)	NM_001622	308	6 373	18 436	26 000
Albumin	AF116645	4 304	30 111	30 234	33 140
	D16931	1 387	23 615	30 668	39 144

†Signal intensity in human genome U133 Plus 2.0 array.

(CT45A5), MAGEA6, four-and-a-half LIM domains 1 (FHL1), Thymosin B4, X-linked (TMSB4X), lectin, galactoside-binding, soluble 1 (LGALS1) and IFN-induced transmembrane protein 2 (IFITM2) – all of which were highly expressed in Li23 cells – and APOA1, AHSG and UGT2B4, which were highly expressed in HuH-7 cells. The remaining five genes were assigned to type C and showed more complex expression profiles (Fig. 2). For instance, Gap junction protein-α 43 kDa (GJA1) expression was observed in HuH-7, HLE, HLF, PLC/PRF/5 and PH5CH8 cell lines, but not in Li23, HuH-6 or HepG2 cell lines. In addition, IGFBP2 expression was observed in Li23, HuH-6 and PH5CH8 cell lines, but not in the other cell lines. Together, these results indicate that the Li23 cell line possesses a distinct expression profile among frequently used hepatic cell lines.

DISCUSSION

IN THIS STUDY, we assigned 17 known genes that showed drastic differences between Li23 and HuH-7 cells, and classified the expression profiles of these genes into at least three types among frequently used hepatic cell lines. Three genes (NY-ESO-1, DEFB1 and LGALS3/Galectin-3) were identified as the representative showing Li23-specific expression.

NY-ESO-1 is a well-characterized cancer-testis antigen (CTAG) that appears to be the most immunogenic CTAG known to date.[14] NY-ESO-1 is expressed in malignant tumors such as melanoma, lung carcinoma and bladder cancer, which are called "CTAG-rich" tumor types, but are expressed solely in the testis among normal adult tissues.[15] Because a spontaneous immune response to NY-ESO-1 is frequently observed in patients with malignant tumors including hepatocellular carcinoma,[16] cancer vaccine trials based on NY-ESO-1 are currently underway.[15] However, the biological role of NY-ESO-1 in both tumors and testis remains poorly understood. Accordingly, the Li23 cell line may be useful for the study of the biological role of NY-ESO-1.

Human defensins, which are small cationic peptides produced by neutrophils and epithelial cells, form two genetically distinct subfamilies, α-defensin and β-defensin. DEFB1, identified in this study, is one of six members belonging to β-defensins and appears to be involved in the antimicrobial defense of the epithelia of surfaces.[16,17] Although α-defensins consisting of six members are known to be expressed in a variety of tumors, DEFB1 is downregulated in some tumor types in which it could behave as a tumor suppressor protein.[18] Our study revealed that except DEFB1 in Li23 cells, no α- or β-defensin members were expressed in the

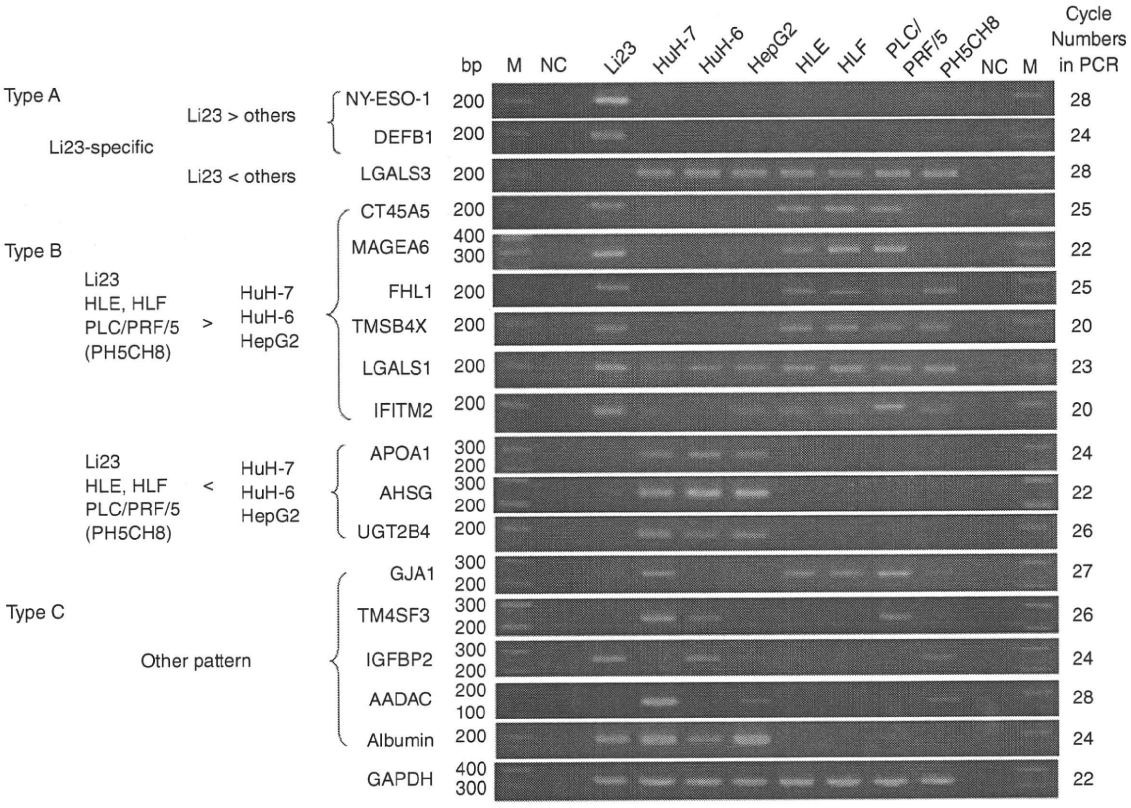

Figure 2 Expression profiles of representative genes, whose expression levels showed drastic differences between Li23 and HuH-7 cells, among human hepatic cell lines. Reverse transcription polymerase chain reaction (RT-PCR) analysis was performed as described in Methods. PCR products were detected by staining with ethidium bromide after separation by electrophoresis on 3% agarose gels.

hepatic cell lines tested in this study (data not shown). Because the molecular mechanism underlying DEFB1 expression or its role in oncogenesis remains to be clarified, Li23 cells may be useful for a study like that.

LGALS3/Galectin-3 is the most studied member of the galectin family, which is characterized by specific binding of β-galactosides through the carbohydrate-recognition domain.[19] LGALS3/Galectin-3 is ubiquitously expressed in numerous cell and tissue types; it is located in both nuclei and cytoplasm, and is secreted through a non-classical pathway. To date, LGALS3/Galectin-3 was found to be involved in many regulations including development, immune reaction, tumorigenesis, and tumor growth and metastasis.[19,20] Indeed, the overexpression of LGALS3/Galectin-3 in cirrhotic and hepatocellular carcinoma has also been reported.[21] In such situations, the absence of LGALS3/Galectin-3 expression in the Li23 cell line is a unique feature among hepatic cell lines, which show high expression levels. Accordingly, the Li23 cell line might be useful as a LGALS3/Galectin-3-null cell line for various studies including those on tumor growth and metastasis.

Although we identified Li23-specific genes showing distinct expression levels among hepatic cell lines examined, microarray analysis revealed that the expression profiles of Li23 and HuH-7 cells, both of which possess an environment for robust HCV replication, differed considerably. Accordingly, such differences may affect the properties or multiplications of HCV, such as susceptibility to anti-HCV reagents, the mutation rate of the HCV genome and the efficiency of HCV replication. Further comparative analysis using Li23 and HuH-7 cells will help to resolve these uncertain subjects.

ACKNOWLEDGMENTS

WE THANK NAOKO Kawahara for her technical assistance. This work was supported by a Grant-in-Aid for research on hepatitis from the Ministry of Health, Labor and Welfare of Japan. K. M. was supported by a Research Fellowship from the Japan Society for Promotion of Science for Young Scientists.

REFERENCES

1 Nakabayashi H, Taketa K, Miyano K, Yamane T, Sato J. Growth of human hepatoma cells lines with differentiated functions in chemically defined medium. *Cancer Res* 1982; **42**: 3858–63.
2 Lohmann V, Körner F, Koch J-O, Herian U, Theilman L, Bartenschlager R. Replication of subgenomic hepatitis C virus RNAs in a hepatoma cell line. *Science* 1999; **285**: 110–13.
3 Wakita T, Pietschmann T, Kato T *et al.* Production of infectious hepatitis C virus in tissue culture from a cloned viral genome. *Nat Med* 2005; **11**: 791–6.
4 Kato N, Sugiyama K, Namba K *et al.* Establishment of a hepatitis C virus subgenomic replicon derived from human hepatocytes infected in vitro. *Biochem Biophys Res Commun* 2003; **306**: 756–66.
5 Ikeda M, Abe K, Dansako H, Nakamura T, Naka K, Kato N. Efficient replication of a full-length hepatitis C virus genome, strain O, in cell culture, and development of a luciferase reporter system. *Biochem Biophys Res Commun* 2005; **329**: 1350–9.
6 Ariumi Y, Kuroki M, Abe K *et al.* DDX3 DEAD-box RNA helicase is required for hepatitis C virus RNA replication. *J Virol* 2007; **81**: 13922–6.
7 Kato N, Mori K, Abe K *et al.* Efficient replication systems for hepatitis C virus using a new human hepatoma cell line. *Virus Res* 2009; **146**: 41–50.
8 Tokiwa T, Doi I, Sato J. Preparation of single cell suspensions from hepatoma cells in culture. *Acta Med Okayama* 1975; **29**: 147–50.
9 Aden DP, Fogel A, Plotkin S, Damjanov I, Knowles BB. Controlled synthesis of HBsAg in a differentiated human liver carcinoma-derived cell line. *Nature* 1979; **282**: 615–16.
10 Doi I, Nambe M, Sato J. Establishment and some biological characteristics of human hepatoma cell lines. *Gann* 1975; **66**: 385–92.
11 Alexander JJ, Bey EM, Geddes EW, Lecatsaa G. Establishment of a continuously growing cell line from primary carcinoma of the liver. *S Afr Med J* 1976; **50**: 2124–8.
12 Ikeda M, Sugiyama K, Mizutani T *et al.* Human hepatocyte clonal cell lines that support persistent replication of hepatitis C virus. *Virus Res* 1998; **56**: 157–67.
13 Dansako H, Naganuma A, Nakamura T, Ikeda F, Nozaki A, Kato N. Differential activation of interferon-inducible genes by hepatitis C virus core protein mediated by the interferon stimulated response element. *Virus Res* 2003; **97**: 17–30.
14 Yoshida N, Abe H, Ohkuri T *et al.* Expression of the MAGE-A4 and NY-ESO-1 cancer-testis antigens and T cell infiltration in non-small cell lung carcinoma and their prognostic significance. *Int J Oncol* 2006; **28**: 1089–98.
15 Caballero OL, Chen YT. Cancer/testis (CT) antigens: potential targets for immunotherapy. *Cancer Sci* 2009; **100**: 2014–21.
16 Korangy F, Ormandy LA, Bleck JS *et al.* Spontaneous tumor-specific humoral and cellular immune responses to NY-ESO-1 in hepatocellular carcinoma. *Clin Cancer Res* 2004; **10**: 4332–41.
17 Bensch KW, Raida M, Magert HJ, Schulz-Knappe P, Forssmann WG. HBD-1: a novel bta-defensin from human plasma. *FEBS Lett* 1995; **368**: 331–5.
18 Droin N, Hendra JB, Ducoroy P, Solary E. Human defensins as cancer biomarkers and antitumour molecules. *J Proteomics* 2009; **72**: 918–27.
19 Dumic J, Dabelic S, Flögel M. Galectin-3: an open-ended story. *Biochim Biophys Acta* 2006; **1760**: 616–35.
20 Danguy A, Camby I, Kiss R. Galectins and cancer. *Biochim Biophys Acta* 2002; **1572**: 285–93.
21 Hsu DK, Dowling CA, Jeng KC, Chen JT, Yang RY, Liu FT. Galectin-3 expression is induced in cirrhotic liver and hepatocellular carcinoma. *Int J Cancer* 1999; **81**: 519–26.

Liver INTERNATIONAL
OFFICIAL JOURNAL OF THE INTERNATIONAL ASSOCIATION FOR THE STUDY OF THE LIVER

Liver International ISSN 1478-3223

BASIC STUDIES

Amino acid substitutions of hepatitis C virus core protein are not associated with intracellular antiviral response to interferon-α *in vitro*

Fusao Ikeda[1,2,3], Hiromichi Dansako[1], Go Nishimura[1], Kyoko Mori[1], Yoshinari Kawai[1,2], Yasuo Ariumi[1], Yasuhiro Miyake[2,3], Akinobu Takaki[2], Kazuhiro Nouso[2,3], Yoshiaki Iwasaki[2], Masanori Ikeda[1], Nobuyuki Kato[1] and Kazuhide Yamamoto[2,3]

1 Department of Tumor Virology, Okayama University Graduate School of Medicine, Dentistry, and Pharmaceutical Sciences, Okayama, Japan
2 Department of Gastroenterology and Hepatology, Okayama University Graduate School of Medicine, Dentistry, and Pharmaceutical Sciences, Okayama, Japan
3 Department of Molecular Hepatology, Okayama University Graduate School of Medicine, Dentistry and Pharmaceutical Sciences, Okayama, Japan

Keywords
antiviral activity – HCV core – hepatitis C virus – interferon

Correspondence
Fusao Ikeda, MD, Department of Gastroenterology and Hepatology, Okayama University Graduate School of Medicine, Dentistry, and Pharmaceutical Sciences, 2-5-1, Shikata-cho, Okayama 700-8558, Japan
Tel: +81 86 235 7219
Fax: +81 86 225 5991
e-mail: fikeda@md.okayama-u.ac.jp

Received 12 March 2010
Accepted 23 May 2010

DOI:10.1111/j.1478-3231.2010.02299.x

Abstract

Background: Studies on patients with hepatitis C virus (HCV) of genotype 1b have suggested that amino acids (aa) 70 and/or 91 of the HCV core protein affect the outcome of interferon (IFN)-α and ribavirin (RBV) therapy, although there are no clear supporting data *in vitro*. *Aims:* This study was designed to determine the differences among the antiviral activities of HCV core proteins with various substitutions at aa70 and/or aa91. *Methods:* The retroviral vectors expressing the HCV core proteins with substitutions of arginine/leucine, arginine/methionine, glutamine/leucine or glutamine/methionine at aa70/aa91 were transiently transfected or stably transducted into an immortalized hepatocyte line (PH5CH8), hepatoma cell lines and an HCV-RNA replicating cell line (sOR) to evaluate antiviral responses to IFN-α or IFN-α/RBV. Sequence analysis was performed using genome-length HCV-RNA replicating cells (OR6 and AH1) to evaluate HCV core mutations during IFN-α treatment. *Results:* The promoter activity levels of IFN-stimulated genes in the transiently transfected cells or the mRNA levels of 2′-5′-oligoadenylate synthetase in the stably transducted PH5CH8 cells were not associated with the HCV core aa70 and/or aa91 substitutions during IFN-α treatment. Antiviral responses to IFN-α or IFN-α/RBV treatment were enhanced in sOR cells stably transducted with the HCV core, although there were no differences in antiviral responses among the cells expressing different core types. Sequence analysis showed no aa mutations after IFN-α treatment. *Conclusions:* Antiviral activities were enhanced by HCV core transduction, but they were not associated with the HCV core aa70 and/or aa91 substitutions by *in vitro* analysis.

Hepatitis C virus (HCV) infection causes chronic hepatitis, and may progress to cirrhosis and hepatocellular carcinoma. More than 170 million people worldwide are infected with HCV, creating a serious global health problem (1, 2). Interferon (IFN)-α is widely used in the treatment of patients with chronic hepatitis C, and the current combination treatment with pegylated IFN-α and ribavirin (RBV) has improved the sustained virological response, and has a success rate of more than 50% (3). Despite this therapeutic success rate, however, there are still non-viral responders (NVR) to IFN-α treatment. High viral load and genotype 1 of HCV are major viral causes of IFN-α resistance. For patients with HCV genotype 1, variations in the amino acid (aa) sequence of the IFN sensitivity-determining region (ISDR) (4) and IFN/RBV resistance-determining region (IRRDR) (5) in the non-structural 5A region have also been reported as important predictors of therapeutic outcomes.

Recent studies on the virological features of HCV patients that are most predictive of NVR to IFN-α/RBV therapy (6, 7) proposed that HCV core protein aa70 and/or aa91 substitutions were independent and significant factors for therapeutic outcomes. In particular, substitutions of arginine by glutamine at aa70 and/or of leucine by methionine at aa91 were common in NVR. Patients with the HCV core aa70 substitutions often had a slow or no decrease in HCV-RNA levels during the early phase of IFN-α treatment (6–9). A previous report evaluating HCV dynamics during IFN-α therapy described a biphasic kinetic pattern of HCV-RNA decline, and the viral

decrease in the first phase was believed to be dependent on the direct effect of IFN-α on infected targets (10). We hypothesized that the types of HCV core proteins might alter the antiviral environment in the infected hepatocytes, and thus the aim of this study was to determine the difference in antiviral effects between HCV core proteins with various aa70 and aa91 substitutions.

Methods

Cell cultures

A non-neoplastic immortalized human hepatocyte line (PH5CH8) and hepatoma cell lines (HepG2, HuH-7 and Li23) were used to evaluate antiviral response, as described previously (11–13). We also used sOR cells harbouring subgenomic HCV-RNA derived from an HCV-O strain (genotype 1b) with Neo and *Renilla* luciferase genes (14). A schematic of the gene organization of sOR cells is shown in Figure 1a. All the cell lines used in this study were reported to possess the normal IFN signalling pathway (13–16). The cells were cultured in Dulbecco's modified Eagle's medium supplemented with 10% fetal bovine serum, penicillin, streptomycin and 0.3 mg/ml of G418 (Geneticin; Invitrogen, Carlsbad, CA, USA).

Plasmid constructions

Four retrovirus pCX4bsr vectors (17) expressing HCV core proteins were constructed, whose aa sequences were identical to the consensus sequences of the HCV core protein from the HCV-O strain encoding aa1–191, except for arginine at aa70/leucine at aa91 for CoreR70L91, glutamine at aa70/leucine at aa91 for CoreQ70L91, glutamine at aa70/methionine at aa91 for CoreQ70M91 and arginine at aa70/methionine at aa91 for CoreR70M91, as shown in Figure 1b. The two types of HCV core protein, CoreQ70L91 and CoreR70L91, were obtained from cells infected with serum HCV-O in a study of the dynamics of HCV populations during culture (18). CoreQ70M91 and CoreR70M91 were constructed from CoreQ70L91 and CoreR70L91, respectively, by PCR mutagenesis with primers containing base alterations. The sequences of these inserts were confirmed by Big Dye termination cycle sequencing using an ABI Prism 310 genetic analyzer (Applied Biosystems, Foster City, CA, USA).

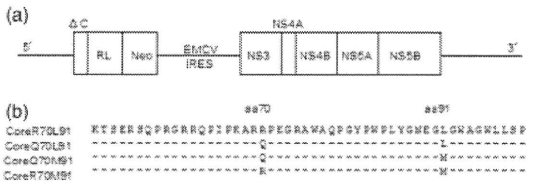

Fig. 1. Schema of subgenomic hepatitis C virus (HCV) RNA and partial aa sequences of the HCV core in the constructed retroviral vectors. (a) A schematic of the gene organization of subgenomic HCV replicon RNA. RL, *Renilla* luciferase; Neo, neomycin phosphotransferase; EMCV IRES, encephalomyocarditis virus internal ribosome entry site. (b) The partial aa sequences of the HCV core protein encoded in the constructed vectors. Four retrovirus pCX4bsr vectors expressing HCV core proteins were constructed, whose aa sequences were identical to the consensus sequences of the HCV core from HCV-O strain encoding aa1–191, except for arginine at aa70/leucine at aa91 for CoreR70L91, glutamine at aa70/leucine at aa91 for CoreQ70L91, glutamine at aa70/methionine at aa91 for CoreQ70M91 and arginine at aa70/methionine at aa91 for CoreR70M91.

Preparation of PH5CH8 cells and sOR cells stably expressing hepatitis C virus core proteins

PH5CH8 cells and sOR cells were infected with retrovirus vectors encoding different types of HCV core proteins, as described previously (19, 20). At 2 days post-infection, the culture medium was exchanged for a fresh medium containing blasticidin (20 μg/ml) for PH5CH8 cells or blasticidin (20 μg/ml) and G418 (0.3 mg/ml) for sOR cells. The culture was continued for 3 weeks so as to select the cells stably expressing the core proteins.

Quantitative reverse transcription-polymerase chain reaction analysis

Total cellular RNA was extracted using an Isogen extraction kit according to the manufacturer's protocol (Nippon Gene, Tokyo, Japan). The quantitative reverse transcription-polymerase chain reaction (RT-PCR) analysis was performed by real-time PCR using a Light Cycler (Roche Diagnostics, Mannheim, Germany) as described previously (20–22).

Luciferase reporter assay

For the dual luciferase assay, we used firefly luciferase reporter vectors encoding the 2′-5′-oligoadenylate synthetase (2′5′OAS) promoter, IFN-induced double-stranded RNA-activated protein kinase (PKR) promoter, IFN-stimulated response element (ISRE), and pRL-CMV, which expressed *Renilla* luciferase as described previously (15, 16). Plasmids were transiently transfected into the cells (2.0×10^4 cells/well in 24-well plates) using the FuGene6 transfection reagent (Roche Diagnostics) and cultured for 48 h. The cells were treated with human IFN-α (Sigma, St Louis, MO, USA) and/or RBV at the indicated doses for 6 h before harvest. The RBV was kindly provided by Yamasa (Chiba, Japan) (23). A whole cell lysate was prepared and assayed for firefly and *Renilla* luciferase activities according to the manufacturer's protocol (Promega, Madison, WI, USA). A Lumat LB9507 luminometer (Berthold, Bad Wildbad, Germany) was used to detect luciferase activity. The relative luciferase activity was normalized to the activity of *Renilla* luciferase. The data represent the means of the normalized luciferase activities of triplicate assays. The protocol for the *Renilla* luciferase assay to quantify HCV replicon

RNA was described previously (14). Briefly, 2.0×10^4 cells were plated onto 24-well plates in triplicate and were cultured for 12 h. The cells were treated with human IFN-α and/or RBV at the indicated doses for 48 h, and then harvested with *Renilla* lysis reagent (Promega) and subjected to a luciferase reporter assay according to the manufacturer's protocol. All the luciferase assays were repeated at least three times.

Western blot analysis

Preparations of cell lysates, sodium dodecyl sulphatepolyacrylamide gel electrophoresis (SDS-PAGE) and immunoblotting were performed as described previously (15, 16). The antibodies used in this study were those against Core (CP-11; Institute of Immunology, Tokyo, Japan), NS3 (Novocastra Laboratories, Newcastle, UK) and β-actin (AC-15; Sigma). Immuno-complexes were detected using the Renaissance enhanced chemiluminescence assay (PerkinElmer Life Science, Boston, MA, USA).

Cell proliferation analysis

The PH5CH8 cells (5.0×10^3 cells/well) or the sOR cells (2.5×10^3 cells/well) stably expressing HCV core proteins were plated onto 96-well plates, cultured for 24, 48 or 72 h and subjected to the colorimetric 3-(4,5-dimethylthiazol-2-yl)-2,5-diphenyltetrazolium bromide (MTT) assay according to the manufacturer's instructions (cell proliferation kit I; Roche) as described previously (24).

Results

No changes in the levels of interferon-stimulated genes were detected in response to the substitutions at hepatitis C virus core amino acid 70 and/or amino acid91 in transiently transfected cells

The constructed plasmids with the four different combinations of HCV core aa70 and aa91 substitutions were transiently transfected into PH5CH8, HepG2, HuH-7 and Li23 cells with lipofection. The levels of 2′5′OAS promoter activities were calculated as the luciferase activities at 48 h after transfection. As shown in Figure 2, the different types of HCV core proteins did not show clear differences in basal levels or enhanced levels with IFN-α stimulation, although the levels of CoreR70L91 transfection were slightly higher than the transfection levels for the other core proteins in PH5CH8 cells. As for PH5CH8 cells, we also evaluated the expression of HCV core proteins with Western blot analysis, and there were no obvious differences as shown in Figure 3. There were no differences either in the levels of the PKR promoter or in ISRE activities (data not shown). These results indicate that the levels of IFN-stimulated genes might not be affected by substitutions of the HCV core proteins at aa70 and/or aa91 in transiently transfected cells.

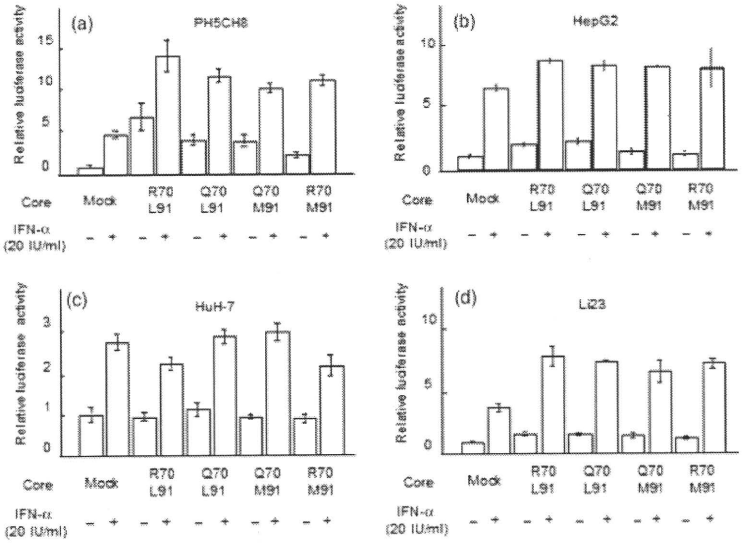

Fig. 2. 2′5′oligoadenylate synthetase (OAS) promoter activity of cells transiently transfected with the hepatitis C virus (HCV) core. The constructed plasmids with the four different types of HCV core aa70 and aa91 were transiently transfected into the cells (2.0×10^4 cells/well in 24-well plates) with lipofection. The cells were treated with IFN-α (20 IU/ml) for 6 h before harvest. The levels of 2′5′OAS promoter activities were calculated as the luciferase activities at 48 h after transfection. The figures show the results using PH5CH8 (a), HepG2 (b), HuH-7 (c) and Li23 cells (d).

Liver International (2010)

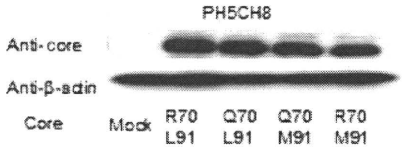

Fig. 3. The expression of hepatitis C virus (HCV) core proteins in the cells transiently transfected with the HCV core. The expressions of HCV core proteins were evaluated with Western blot analysis for PH5CH8. The constructed plasmids with the four different types of HCV core aa70 and aa91 were transiently transfected into the cells (2.0×10^5 cells/well in six-well plates) with lipofection. The cells were collected at 48 h after transfection.

The intracellular antiviral activities were augmented by hepatitis C virus core transduction, although they might not be affected by the amino acid 70 and/or amino acid 91 substitutions in the hepatitis C virus core stably transducted cells

To evaluate the interaction between the stable expression of HCV core proteins and intracellular antiviral activity, we prepared PH5CH8 cells that stably expressed HCV core proteins with retroviral transduction. The 2′5′OAS mRNA levels were measured with real-time LightCycler PCR and normalized with β-actin mRNA levels. As shown in Figure 4a, there were no clear differences in the basal levels or IFN-α-enhanced levels among the four transducted cell lines and the mock-transducted cells, although the expression levels of HCV core protein stably transducted cells were slightly higher than that of mock-induced cells. Western blot analysis showed that all these cell lines had similar levels of HCV core proteins (data not shown). Next, we monitored the association between the stable expression of HCV core proteins and RNA replication in an HCV replicon system. As we considered that a small difference of antiviral activity might be difficult to detect with real-time PCR, sOR cells were used for the monitoring. These cells are subgenomic HCV-RNA replicating cells with *Renilla* luciferase genes, and the replicon RNA can be quantified as luciferase activity. Measurement of luciferase activity is a useful and accurate means of quantifying the replicon RNA, because its sensitivity is much better than that of real-time PCR (14). We prepared the sOR cells expressing the HCV core proteins with retroviral transduction and stimulated the cells with IFN-α for 48 h. The level of antiviral activity, which was calculated as the median effective concentration (EC_{50}) of IFN-α, demonstrated that the cells transducted with the HCV core proteins showed a better response to IFN-α stimulation, but there was no difference in response among the cells expressing the different types of HCV core proteins, which is consistent with the results for the transient transfection of HCV core proteins (Fig. 4b). Western blot analysis demonstrated that the expressions of the HCV core and NS3 proteins did not show a clear difference among the sOR cells, irrespective of the types of HCV core proteins (Fig. 4c). As shown in Figure 4d, the results of the MTT assay demonstrated that the expressions of different types of HCV core proteins were not associated with cell proliferation in PH5CH8 cells or sOR cells. These results indicate that the intracellular antiviral activities are augmented in the presence of HCV core proteins, but they are not altered by the different substitutions at HCV core aa70 and/or aa91 in the cells stably expressing the HCV core.

Co-stimulation of interferon-α with ribavirin did not alter the association of hepatitis C virus core proteins with intracellular antiviral activity

Next, we hypothesized that co-stimulation of RBV might modulate the antiviral activity of the cells with different types of HCV core proteins. As shown in Figure 5, we evaluated the antiviral activity by quantifying HCV replicon RNA and 2′5′OAS promoter activity in the presence of IFN-α and RBV. The dose of RBV (20 μM) was determined based on the clinically used dose and the cell reactivity to RBV in our previous report (23). The HCV replications were suppressed (Fig. 5a), and the levels of 2′5′OAS promoter activities were enhanced (Fig. 5b and c) with a smaller dose of IFN-α, compared with IFN-α stimulation alone, indicating that RBV exerted an additive effect. Interestingly, the stimulation with RBV alone did not show any enhancement of 2′5′OAS promoter activity. These results indicate that the intracellular antiviral activities are augmented by costimulation with IFN-α with RBV, and that they are not altered by changes in the HCV core aa70 and/or aa91 substitutions.

Specific amino acid substitutions of hepatitis C virus core proteins were not detected in response to interferon-α treatment in the genome-length hepatitis C virus-RNA replicating cells

Next, we hypothesized that specific mutations in the HCV core region occur during IFN-α treatment. The two kinds of genome-length HCV-RNA replicating cells with different core aa70 and aa91 substitutions were cultured for 3 weeks with low-dose IFN-α stimulation, and then the core sequences were compared. We used OR6 and AH1 cells, both of which are genome-length HCV-RNA replicating cells (25, 26). OR6 cells have core proteins with glutamine at aa70 and leucine at aa91, corresponding to CoreQ70L91. AH1 cells have core proteins with arginine at aa70 and leucine at aa91, corresponding to CoreR70L91. After 3 weeks of culture with 12.5 IU/ml of IFN-α, several IFN-α- and G418-resistant colonies were obtained. We cultured them further without IFN-α stimulation and spread the colonies individually on 24-well plates. To examine the aa sequences of the core proteins in the colonies derived from OR6 and AH1 cells, RT-PCR was performed for the region encoding the HCV core protein, and the obtained PCR products were cloned into pBlueScript II, as described previously (27). The plasmid inserts of 10 clones each were sequenced. The results revealed that there were no specific changes of the aa sequence of HCV core

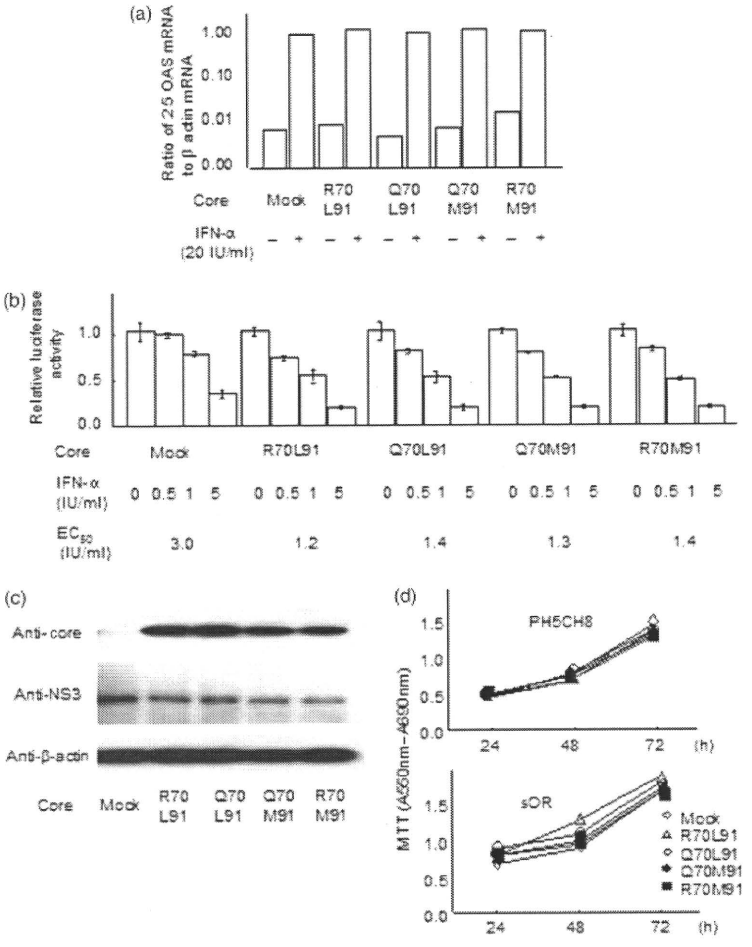

Fig. 4. Antiviral activity of cells stably transducted with hepatitis C virus (HCV) core proteins. The antiviral activity of PH5CH8 cells stably transducted with the HCV core were evaluated by 2′5′oligoadenylate synthetase (OAS) mRNA levels (a). The cells (2.0×10^5/well in six-well plates) were cultured for 48 h, and treated with IFN-α (20 IU/ml) for 6 h before harvest. 2′5′OAS mRNA levels were measured with real-time LightCycler PCR and normalized with β-actin mRNA levels. The sOR cells stably expressing the different types of HCV core (2.0×10^4 cells/well in 24-well plates) were stimulated with IFN-α for 48 h, and the HCV RNA levels of the cells were calculated as the percent relative *Renilla* luciferase activity [relative RL activity (%)] and compared by evaluating the EC_{50} of IFN-α (b). sOR cells stably transducted with the HCV core (2.0×10^5/well in six-well plates) were cultured for 48 h, and prepared for Western blot analysis with anti-core, anti-NS3 or anti-β-actin antibody (c). The PH5CH8 cells (5.0×10^3 cells/well) or the sOR cells (2.5×10^3 cells/well) stably expressing HCV core proteins were plated onto 96-well plates, cultured for 24, 48 or 72 h and subjected to MTT assay. The results for PH5CH8 cells are shown in the upper panel of Figure 4d and those for sOR cells are shown in the lower panel.

proteins from that of the original cells. The OR6 cells retained glutamine at aa70 and leucine at aa91, while the AH1 cells retained arginine at aa70 and leucine at aa91. These results suggest that the aa at positions 70 and 91 are stable during IFN-α treatment.

Discussion

Recent studies on HCV-infected patients have suggested that HCV core proteins with substitutions at aa70 and/or aa91 may be significantly associated with NVR to IFN-α/RBV therapy, and that patients with aa70 substitutions of arginine to glutamine often have slow or no decrease in HCV-RNA levels during the early phase of IFN-α treatment (6–9). However, the associations between HCV core aa70 and/or aa91 substitutions and the level of antiviral activity have not been determined *in vitro*. We hypothesized that the aa at the HCV core positions 70 and/or 91 would be associated with the intracellular antiviral environment in HCV-infected cells, and

Liver International (2010)

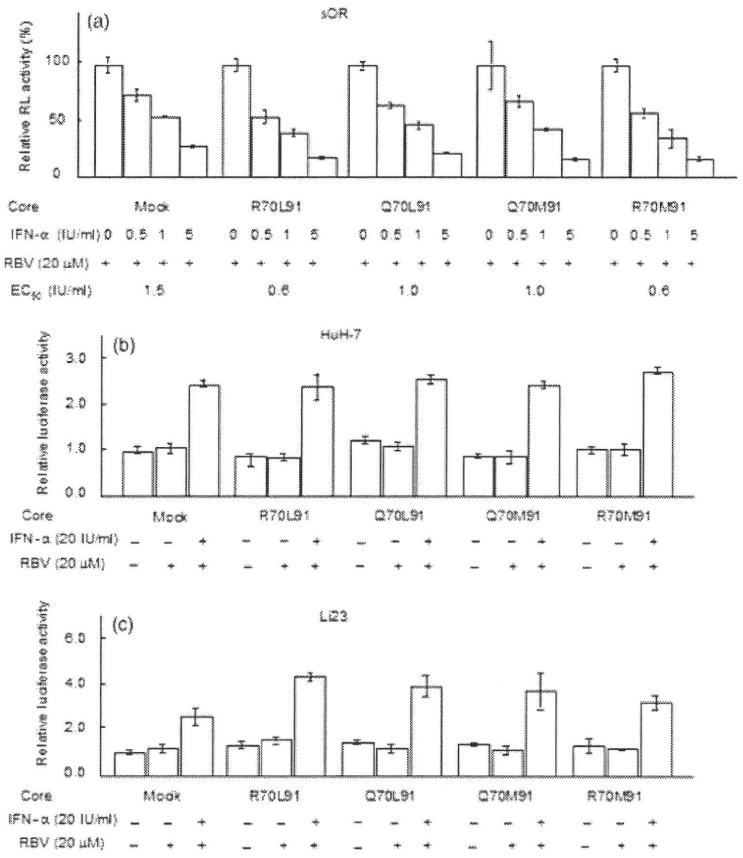

Fig. 5. Antiviral activity with stimulation of interferon (IFN)-α in combination with ribavirin (RBV). The sOR cells (2.0×10^4 cells/well in 24-well plates) stably expressing the different types of HCV core were stimulated with the indicated doses of IFN-α and 20 μM of RBV for 48 h, and the hepatitis C virus (HCV) RNA levels of the cells were calculated as the percent relative *Renilla* luciferase activity [relative RL activity (%)]. The EC_{50} of IFN-α was calculated as shown in (a). HuH-7 cells and Li23 cells were seeded (2.0×10^4 cells/well in 24-well plates), and the different types of HCV core were transiently transfected into the cells with lipofection. The transfected cells were treated with 20 IU/ml of IFN-α and 20 μM of RBV for 6 h before harvest. The levels of 2′5′oligoadenylate synthetase promoter activities were calculated as the luciferase activities after 48 h of transfection. The figures show the results using HuH-7 cells (b) and Li23 cells (c).

evaluated the differences in IFN-α-induced antiviral activities according to the aa at these positions. Our results suggest that differences in the aa at HCV core positions 70 and/or 91 are not associated with the intracellular antiviral activity in HCV-infected cells.

The HCV core protein has been reported to exert an effect on a variety of cellular functions, including apoptosis, RNA metabolic processes, inflammation, cholesterol metabolism and protein catabolism (1, 28–32), and is currently considered to play important roles in persistent infection. In terms of a direct interaction between the HCV core protein and antiviral activity, Naganuma *et al.* (15) reported that 2′5′OAS promoter activity was activated in PH5CH8 cells when the cells were transiently transfected with the HCV core protein, and their deletion mutant analysis indicated that HCV core aa70 and/or aa91 substitutions were not associated with activated 2′5′OAS promoter activity, which is consistent with our present results that the antiviral activities were not associated with the aa at the core position 70 or 91 in the transiently transfected cells. Furthermore, we evaluated the antiviral activity in cells stably transducted with the HCV core protein by precisely measuring the levels of HCV replicon RNA based on luciferase activity. For this purpose, we used sOR cells, which are subgenomic HCV-RNA-replicating cells. The sOR cells facilitates the monitoring of HCV replication, although it lacks the steps of budding or HCV re-infection to other cells. Future studies will be required to assess these steps according to the different substitutions at HCV core aa70 and/or aa91, and infectious HCV production systems from the HCV genotype 1b strain will be required for this purpose.

It is not clear whether the aa at the core positions 70 or 91 can be changed through IFN-α therapy or disease progression. Our results revealed that the aa at the core positions 70 or 91 in the cells with monoclonal HCV replication were not substituted after 3 weeks of IFN-α treatment. The substitution of arginine to glutamine at aa70, or of leucine to methionine at aa91 might not occur in the infected cells, but rather through a change in the dominant virus, such as through resistance to IFN-α therapy or during disease progression.

In conclusion, the antiviral activities in response to IFN-α or IFN-α/RBV treatment were augmented by HCV core transduction. However, the levels of these activities were not associated with changes in the aa at HCV core positions 70 or 91 by *in vitro* analysis with immortalized hepatocytes or HCV-RNA replicating cells.

References

1. Kato N. Molecular virology of hepatitis C virus. *Acta Med Okayama* 2001; **55**: 133–59.
2. Thomas DL. Hepatitis C epidemiology. *Curr Top Microbiol Immunol* 2000; **242**: 25–41.
3. Firpi RJ, Nelson DR. Current and future hepatitis C therapies. *Arch Med Res* 2007; **38**: 678–90.
4. Enomoto N, Sakuma I, Asahina Y, *et al.* Comparison of genome-length sequences of interferon-sensitive and resistant hepatitis C virus 1b. Sensitivity to interferon is conferred by amino acid substitutions in the NS5A region. *J Clin Invest* 1995; **96**: 224–30.
5. El-Shamy A, Nagano-Fujii M, Sasase N, *et al.* Sequence variation in hepatitis C virus nonstructural protein 5A predicts clinical outcome of pegylated interferon/ribavirin combination therapy. *Hepatology* 2008; **48**: 38–47.
6. Akuta N, Suzuki F, Sezaki H, *et al.* Association of amino acid substitution pattern in core protein of hepatitis C virus genotype 1b high viral load and non-virological response to interferon–ribavirin combination therapy. *Intervirology* 2005; **48**: 372–80.
7. Donlin MJ, Cannon NA, *et al.* Virahep-C Study Group. Pretreatment sequence diversity differences in the genome-length hepatitis C virus open reading frame correlate with early response to therapy. *J Virol* 2007; **81**: 8211–24.
8. Akuta N, Suzuki F, Kawamura Y, *et al.* Predictors of viral kinetics to peginterferon plus ribavirin combination therapy in Japanese patients infected with hepatitis C virus genotype 1b. *J Med Virol* 2007; **79**: 1686–95.
9. Akuta N, Suzuki F, Kawamura Y, *et al.* Predictive factors of early and sustained responses to peginterferon plus ribavirin combination therapy in Japanese patients infected with hepatitis C virus genotype 1b: amino acid substitutions in the core region and low-density lipoprotein cholesterol levels. *J Hepatol* 2007; **46**: 403–10.
10. Neumann AU, Lam NP, Dahari H, *et al.* Hepatitis C viral dynamics in vivo and the antiviral efficacy of interferon-alpha therapy. *Science* 1998; **282**: 103–7.
11. Ikeda M, Sugiyama K, Mizutani T, *et al.* Human hepatocyte clonal cell lines that support persistent replication of hepatitis C virus. *Virus Res* 1998; **56**: 157–67.
12. Noguchi M, Hirohashi S. Cell lines from non-neoplastic liver and hepatocellular carcinoma tissue from a single patient. *In Vitro Cell Dev Biol Anim* 1996; **32**: 135–7.
13. Kato N, Mori K, Abe K, *et al.* Efficient replication systems for hepatitis C virus using a new human hepatoma cell line. *Virus Res* 2009; **146**: 41–50.
14. Nishimura G, Ikeda M, Mori K, *et al.* Replicons from genotype 1b HCV-positive sera exhibit diverse sensitivities to anti-HCV reagents. *Antiviral Res* 2009; **82**: 42–50.
15. Akagi T, Sasai K, Hanafusa H. Refractory nature of normal human diploid fibroblasts with respect to oncogene-mediated transformation. *Proc Natl Acad Sci USA* 2003; **100**: 13567–72.
16. Kato N, Ikeda M, Sugiyama K, *et al.* Hepatitis C virus population dynamics in human lymphocytes and hepatocytes infected in vitro. *J Gen Virol* 1998; **79**: 1859–69.
17. Naganuma A, Dansako H, Nakamura T, Nozaki A, Kato N. Promotion of microsatellite instability by hepatitis C virus core protein in human non-neoplastic hepatocyte cells. *Cancer Res* 2004; **64**: 1307–14.
18. Dansako H, Ikeda M, Kato N. Limited suppression of the interferon-beta production by hepatitis C virus serine protease in cultured human hepatocytes. *FEBS J* 2007; **274**: 4161–76.
19. Abe K, Ikeda M, Dansako H, *et al.* cDNA microarray analysis to compare HCV subgenomic replicon cells with their cured cells. *Virus Res* 2005; **107**: 73–81.
20. Dansako H, Naka K, Ikeda M, Kato N. Hepatitis C virus proteins exhibit conflicting effects on the interferon system in human hepatocyte cells. *Biochem Biophys Res Commun* 2005; **336**: 458–68.
21. Naganuma A, Nozaki A, Tanaka T, *et al.* Activation of the interferon inducible 2′-5′-oligoadenylate synthetase gene by hepatitis C virus core protein. *J. Virol* 2000; **74**: 8744–50.
22. Dansako H, Naganuma A, Nakamura T, *et al.* Differential activation of interferon-inducible genes by hepatitis C virus core protein mediated by the interferon stimulated response element. *Virus Res* 2003; **97**: 17–30.
23. Naka K, Ikeda M, Abe K, Dansako H, Kato N. Mizoribine inhibits hepatitis C virus RNA replication: effect of combination with interferon-alpha. *Biochem Biophys Res Commun* 2005; **330**: 871–9.
24. Kuroki M, Ariumi Y, Ikeda M, *et al.* Arsenic trioxide inhibits hepatitis C virus RNA replication through modulation of the glutathione redox system and oxidative stress. *J Virol* 2009; **83**: 2338–48.
25. Ikeda M, Abe K, Dansako H, *et al.* Efficient replication of a genome-length hepatitis C virus genome, strain O, in cell culture, and development of a luciferase reporter system. *Biochem Biophys Res Commun* 2005; **329**: 1350–9.
26. Mori K, Abe K, Dansako H, *et al.* New efficient replication system with hepatitis C virus genome derived from a patient with acute hepatitis C. *Biochem Biophys Res Commun* 2008; **371**: 104–9.

Liver International (2010)

27. Alam SS, Nakamura T, Naganuma A, *et al.* Hepatitis C virus quasispecies in cancerous and noncancerous hepatic lesions: the core protein-encoding region. *Acta Med Okayama* 2002; **56**: 141–7.
28. Lai MM, Ware CF. Hepatitis C virus core protein: possible roles in viral pathogenesis. *Curr Top Microbiol Immunol* 2000; **242**: 117–34.
29. Ariumi Y, Kuroki M, Abe K, *et al.* DDX3 DEAD-box RNA helicase is required for hepatitis C virus RNA replication. *J Virol* 2007; **81**: 13922–6.
30. Waris G, Felmlee DJ, Negro F, Siddiqui A. Hepatitis C virus induces proteolytic cleavage of sterol regulatory element binding proteins and stimulates their phosphorylation via oxidative stress. *J Virol* 2007; **81**: 8122–30.
31. Joo M, Hahn YS, Kwon M, *et al.* Hepatitis C virus core protein suppresses NF-kappaB activation and cyclooxygenase-2 expression by direct interaction with IkappaB kinase beta. *J Virol* 2005; **79**: 7648–57.
32. Osna NA, White RL, Krutik VM, *et al.* Proteasome activation by hepatitis C core protein is reversed by ethanol-induced oxidative stress. *Gastroenterology* 2008; **134**: 2144–52.

Journal of Bioscience and Bioengineering
VOL. 110 No. 3, 374–376, 2010

ELSEVIER

www.elsevier.com/locate/jbiosc

TECHNICAL NOTE

Generation of single-chain Fvs against detergent-solubilized recombinant antigens with a simple coating procedure

Torahiko Tanaka,[1,*] Yuichiro Hasegawa,[2,3] Makoto Saito,[2,3] Masanori Ikeda,[4] and Nobuyuki Kato[4]

Department of Advanced Medical Science, Nihon University School of Medicine, 30-1 Oyaguchi-kamimachi, Itabashi, Tokyo 173-8610, Japan[1]
Department of Obstetrics and Gynecology, Nihon University School of Medicine, 30-1 Oyaguchi-kamimachi, Itabashi, Tokyo 173-8610, Japan[2]
Open Research Center for Genome and Infectious Disease Control, Nihon University School of Medicine, 30-1 Oyaguchi-kamimachi, Itabashi, Tokyo 173-8610, Japan[3] *and Department of Tumor Virology, Okayama University Graduate School of Medicine, Dentistry, and Pharmaceutical Sciences, 2-5-1 Shikata-cho, Okayama 700-8558, Japan*[4]

Received 5 February 2010; accepted 29 March 2010

Antigen coating on polystyrene is prevented by detergent. We present here a simple procedure to coat detergent-solubilized antigen for subsequent panning selection of single-chain Fv (scFv), the target antigen of which was the hepatitis C virus (HCV) non-structural protein (NS) 4B, an integral membrane protein.

[**Key words:** Single-chain Fv; Detergent; Critical micelle concentration; Hepatitis C virus; NS4B]

The single-chain Fv (scFv)-phage display (1) is a useful technology to obtain antibodies against a wide category of antigens, including non-protein antigens, autoantigens, and antigens that are difficult to generate in animals. To obtain specific scFvs, panning selection has been performed on antigen-coated polystyrene using an scFv-phage display library (2). Antigen coating is achieved by the simple incubation of a soluble antigen solution in polystyrene tubes and wells. However, when an antigen is detergent-solubilized, detergent severely disturbs antigen coating on polystyrene (3,4) and this becomes an obstacle to the panning selection of scFv. To overcome the problem, we developed a simple procedure to coat an antigen by lowering the detergent concentration in an antigen solution with no additional material or time-consuming work. The target antigen was the hepatitis C virus (HCV) non-structural protein (NS) 4B, an integral membrane protein. HCV has a positive-stranded RNA genome encoding at least 10 viral proteins, namely, a core, E1, E2, p7, NS2, NS3, NS4A, NS4B, NS5A, and NS5B (5). The 5' untranslated region has a functional internal ribosome entry site, and the 3' untranslated region contains a highly conserved 98 nucleotide structure, the 3' X (6), which is indispensable for the viral genome replication. The NS proteins are thought to form complexes to replicate the viral genome. Little is known about the role of NS4B which harbors at least four transmembrane domains. Anti-NS4B scFvs to various epitopes are a useful tool for analyzing the roles of NS4B in virus replication.

We prepared the N-terminal hexahistidine (His)-tagged NS4B (NS4BHis) as an antigen based on the sequence of strain O (subtype 1b HCV) (7) using the pET expression system (Novagen, USA). The NS4B fragment was amplified by PCR using the restriction-site-tagged primers 5'-TTACATATGCATCACCACCATCACCATGGTGCCTCGCACC-TCCCTTAC-3' (with the *Nde*I site as underlined) and 5'-TTAGGATCCT-TAGCATGGCGTGGAGCAGTC-3' (with the *Bam*HI site as underlined) with a plasmid pON/C-5B/KE (7) as a template. The expression construct was created by ligating the *Nde*I–*Bam*HI-digested fragment of NS4B into the *Nde*I–*Bam*HI-digested pET3a vector. Similarly, the N-terminal Myc (EQKLISEEDL)-His-tagged NS4B (NS4BMycHis) construct was created by PCR using the primers 5'-TTACATATGGAACA-GAAACTGATTAGCGAAGAAGATCTGCATCACCACCATCACCATG-3' (with the *Nde*I site as underlined) and 5'-TTAGGATCCTTAGCATGGCGTGGAG-CAGTC-3' (with the *Bam*HI site as underlined) with the NS4BHis construct as the PCR template. NS4B proteins were expressed in *Escherichia coli* strain KRX (Promega, USA) in the presence of 0.1% rhamnose at 25 °C. The cells were suspended in a buffer containing 10 mM Tris–HCl, pH 7.4, 5 mM EDTA, and a Complete™ protease inhibitor cocktail (Roche, Germany), sonicated three times with 5 s bursts, and centrifuged at 5000*g* for 3 min. Because NS4BHis was recovered in the pellet, the solubilization conditions were examined. NS4BHis was efficiently solubilized in the presence of 0.5 M NaCl with 1% n-dodecyl β-D-maltoside (DDM) or Triton X-100 but not with Tween-20 and n-octyl β-D-glucoside (OG). After solubilization with DDM, NS4BHis was affinity-purified using Ni NTA agarose (Qiagen, USA) to near-homogeneity according to the manufacturer's protocol.

In the usual panning selection of antigen-specific scFv, the antigen is coated on polystyrene by simple incubation in an aqueous buffer. In the present work, the purified NS4BHis preparation contains 1% DDM, and, as described above, detergents are known to severely disturb antigen coating on polystyrene. Upon a preliminary experiment, we failed to efficiently coat NS4BHis with 50-fold simple dilution (final

* Corresponding author. Present address: Division of Biochemistry, Department of Biomedical Sciences, Nihon University School of Medicine, 30-1 Oyaguchi-kamimachi, Itabashi, Tokyo 173-8610, Japan. Tel.: +81 3 3972 8111x2241; fax: +81 3 3972 8199.
E-mail address: tanakat@med.nihon-u.ac.jp (T. Tanaka).

1389-1723/$ - see front matter © 2010, The Society for Biotechnology, Japan. All rights reserved.
doi:10.1016/j.jbiosc.2010.03.014

DDM, 0.02%) on polystyrene. We then modified the purification step to lower the DDM concentration. After NS4BHis was bound to Ni affinity resin, washing and elution were conducted using a buffer with a low but slightly higher than critical micelle concentration (CMC) of DDM (0.01%; the CMC of DDM is 0.0087%). In detail, the Ni affinity resin was pre-equilibrated with a TBS buffer (10 mM Tris–HCl, pH 7.4, 0.15 M NaCl) containing 0.01% DDM and 20 mM imidazole, and the solubilized NS4BHis sample (to which 20 mM imidazole was also added) was applied to the resin. The bound NS4BHis was washed first with a 10-bed volume of the same buffer for equilibration and then with a 10-bed volume of TBS-0.01% DDM-0.5 M NaCl-20 mM imidazole, pH 7.4. Finally, the bound NS4B was eluted with a three-bed volume of TBS-0.01% DDM-0.5 M NaCl-0.25 M imidazole, pH 7.4. Under these conditions, NS4BHis could be purified and concentrated efficiently. Interestingly, even with 0.005% DDM, NS4BHis was efficiently purified in a similar manner. By further 50-fold dilution with a detergent-free buffer (final DDM concentration, 0.0002%), the NS4BHis was found to be coated on polystyrene efficiently. Thus a simple coating protocol for detergent-solubilized antigens was established by a modification of purification procedure to lower detergent concentrations.

We examined the concentration limits of frequently used detergents, including DDM, which enable the coating of NS4BHis (Fig. 1). For this purpose, NS4BMycHis was prepared using the same purification protocol as for NS4BHis with 0.01% of DDM. The NS4BMycHis solution was incubated in polystyrene wells in a microtiter plate with or without various concentrations of detergent (NP40, Triton X-100, Tween-20, OG, and DDM). In this experiment, a 1 µl (2.5 µg) purified NS4BMycHis preparation containing 0.01% DDM was diluted to 50 µl with a TBS buffer for each well; thus, the coating solution contained 0.0002% of carry-over DDM. After 6 h of incubation, each well was blocked, and the amount of adsorbed NS4BMycHis was evaluated using an anti-myc antibody HRP conjugate and the peroxidase-dependent colorimetric

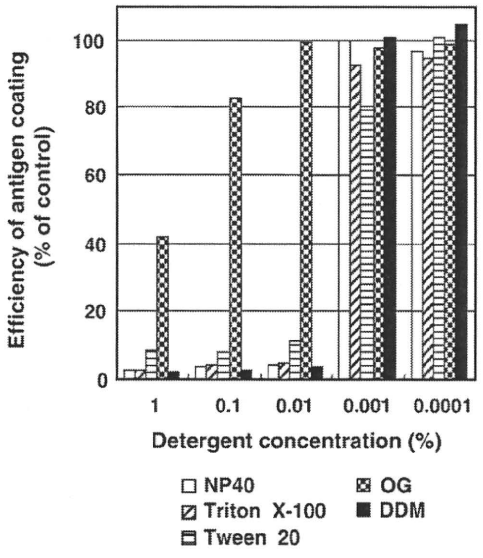

FIG. 1. The influence of various detergents on the coating of NS4B to microplate wells. All the reactions were carried out with final volume of 50 µl in microplate wells (Iwaki, Japan). NS4BMycHis (2.5 µg) was incubated for 6 h at room temperature in the absence or presence of an indicated concentration of detergent (NP 40, Triton X-100, Tween 20, OG, or DDM). The wells were washed 10 times with ultrapure water and blocked with a 5% skim milk-TBS buffer (MTBS) for 1 h. After washing, the wells were reacted with 200-fold diluted anti-myc antibody HRP conjugate (Wako Chemical, Japan) in 5% MTBS for 1 h. After washing, the wells were reacted with 2, 2'-azino-bis(3-ethylbenzthiazoline-6-sulfonic acid) (ABTS; Sigma, USA) according to manufacturer's protocol and the absorbance at 405 nm was determined. Data are the mean of two independent experiments and shown as a % of the control value obtained in the absence of detergent.

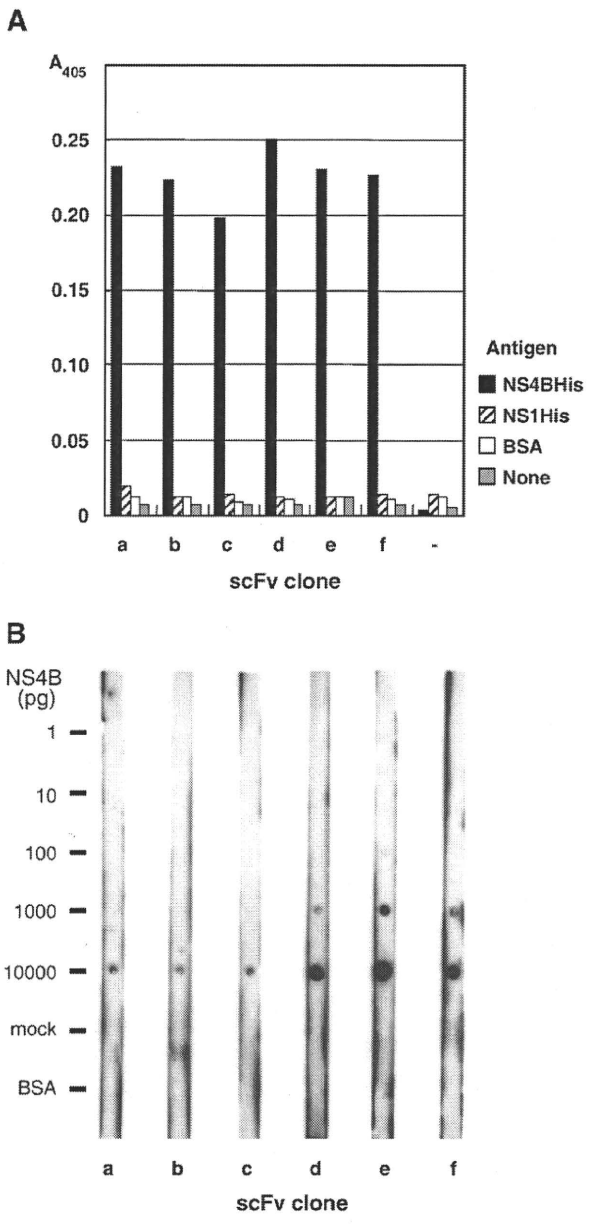

FIG. 2. Specificity and sensitivity assays of scFv phage clones against NS4B. (A) Confirmation of the antigen specificity by ELISA. All the reactions were carried out with final volume of 50 µl in each well. Indicated antigens (1 µg in TBS buffer); NS4BHis (containing 0.0002% DDM as final concentration), influenza virus NS1His (8), and bovine serum albumin (BSA) or TBS buffer alone (None), were incubated in wells of a microplate at 4 °C overnight. The wells were washed 10 times with ultrapure water and blocked with a 5% MTBS for 1 h. The wells were then incubated with or without (−) phage clones (a to f, 2.5×10^9 cfu in 5% MTBS) for 1 h, followed by incubation with 10,000-fold dilution of anti-M13 antibody HRP conjugate (GE, USA) in 5% MTBS for 30 min. Reaction was developed with ABTS and the absorbance at 405 nm was determined. (B) A sensitivity assay of scFv clones against NS4B. Indicated amounts of NS4BHis (0 [mock], 1, 10, 100, 1000, and 10,000 pg) and BSA (10 ng) in 0.5 µl TBS-0.01% DDM were spotted on nitrocellulose strips, air-dried, and incubated in TBS-0.1% Tween-20 overnight. After washing with ultrapure water, the spots were blocked, reacted with scFv phage (5×10^{10} cfu/ml in 5% MTBS) for 1 h, and visualized using an anti-M13 antibody HRP (horseradish peroxidase) conjugate and the ECL-Plus Western Blotting Detection Kit (GE Healthcare, UK) as described previously (9,11).